BIOCHEMISTRY
including biophysical chemistry & molecular biology

Accelerated Publication

pubs.acs.org/biochemistry

Molecular Basis of Recognition of Antibacterial Porphyrins by Heme-Transporter IsdH-NEAT3 of *Staphylococcus aureus*

Yoshitaka Moriwaki,[†] Jose M. M. Caaveiro,*[,†] Yoshikazu Tanaka,[‡] Hiroshi Tsutsumi,[§] Itaru Hamachi,[§] and Kouhei Tsumoto*[,†]

[†]Medical Proteomics Laboratory, Institute of Medical Science, The University of Tokyo, Minato-ku, Tokyo 108-8639, Japan

[‡]Creative Research Institute "Sousei", Hokkaido University, Sapporo 001-0021, Japan

[§]Department of Synthetic Chemistry and Biological Chemistry, Kyoto University, Katsura, Nishikyo-Ku, Kyoto 615-8510, Japan

Supporting Information

ABSTRACT: Antibiotic resistance is increasingly seen as a serious problem that threatens public health and erodes our capacity to effectively combat disease. So-called non-iron metalloporhyrins have shown promising antibacterial properties against a number of pathogenic bacteria including *Staphylococcus aureus*. However, little is known about the molecular mechanism(s) of action of these compounds and in particular how they reach the interior of the bacterial cells. A popular hypothesis indicates that non-iron metalloporphyrins infiltrate into bacterial cells like a "Trojan horse" using heme transport systems. Iron-regulated surface determinant (Isd) is the best characterized heme transport system of *S. aureus*. Herein we studied the molecular mechanism by which the extracellular heme-receptor IsdH-NEAT3 of Isd recognizes antimicrobial metalloporphyrins. We found that potent antibacterial porphyrins Ga(III)-protoporphyrin IX (PPIX) and Mn(III)-PPIX closely mimicked the properties of the natural ligand heme, namely (i) stable binding to IsdH-NEAT3 with comparable affinities for the receptor, (ii) nearly undistinghuishable three-dimensional structure when complexed with IsdH-NEAT3, and (iii) similar transfer properties to a second receptor IsdA. On the contrary, weaker antibacterial porphyrins Mg(II)-PPIX, Zn(II)-PPIX, and Cu(II)-PPIX were not captured effectively by IsdH-NEAT3 under our experimental conditions and displayed lower affinities. Moreover, reduction of Fe(III)-PPIX to Fe(II)-PPIX with dithionite abrogated stable binding to receptor. These data revealed a clear connection between oxidation state of metal and effective attachment to IsdH-NEAT3. Also, the strong correlation between binding affinity and reported antimicrobial potency suggested that the Isd system may be used by these antibacterial compounds to gain access to the interior of the cells. We hope these results will increase our understanding of Isd system of *S. aureus* and highlight its biomedical potential to deliver new and more efficient antibacterial treatments.

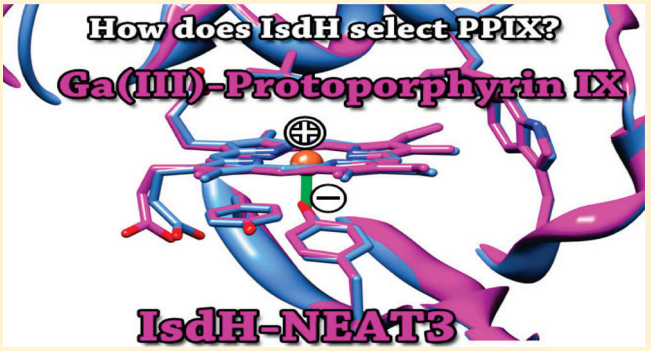

Staphylococcus aureus is a commensal organism that colonizes the anterior nares and skin of about 20−50% of the human population.[1−3] Although its pathogenicity is largely suppressed in healthy people, *S. aureus* can cause various life-threatening disorders such as endocarditis, pneumonia, and septicemia in immune-depressed individuals.[4−6] More worrisome is the fact that strains of *S. aureus* are gaining resistance against antibiotics of last resort such as vancomycin[7] and methicillin.[8] Development of novel drugs and/or vaccines is a necessary step to reduce the increasing risks posed by this bacterium to public health. It is thus desirable to expand the repertoire of essential metabolic pathways at which to aim novel and more sophisticated antibacterial strategies.

So-called iron-regulated surface determinant (Isd) is an attractive target against *S. aureus* because its inactivation would interfere with the ability of the bacterium to acquire iron deemed essential for growth.[9−11] The Isd system comprises nine protein receptors and transporters that extract, transport, and degrade heme molecules from the host organism in order to utilize, for its own metabolic needs, the iron atom contained in the heme group (Figure S1).[12−14] In the first step, heme is captured by extracellular IsdH or IsdB receptors attached to the cell wall. Heme is subsequently transferred to the membrane complex IsdEF·FhuD (function of membrane protein IsdD is still unknown) via intermediate transporters IsdA and IsdC. A common feature among Isd proteins residing in the cell wall (i.e., IsdH, IsdA, IsdB, IsdC) is that all of them possess one or more NEAr transporter (NEAT) domains. In particular, extracellular receptor IsdH possesses three such domains. NEAT1 and NEAT2 bind hemoglobin (major carrier of heme molecules in host organism),[15] whereas NEAT3 domain (IsdH-NEAT3) captures heme molecules extracted from hemoglobin and subsequently transfers them to downstream receptors such

Received: April 1, 2011
Published: July 28, 2011

dx.doi.org/10.1021/bi200493h | *Biochemistry* 2011, 50, 7311−7320

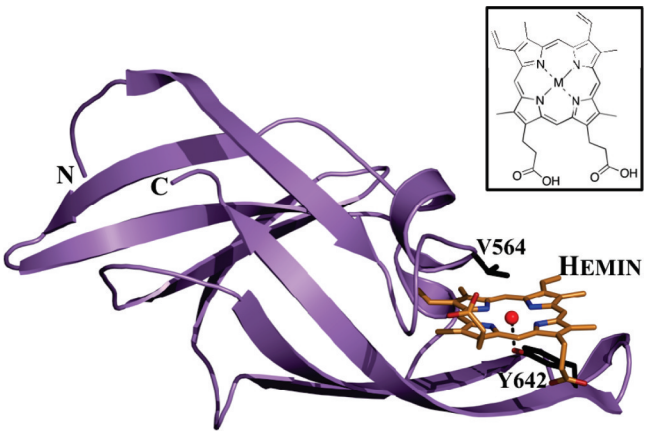

Figure 1. Crystal structure of IsdH-NEAT3 in complex with Fe(III)-PPIX. Coordinates were obtained from entry number 2Z6F of the Protein Data Base.[16] Secondary structure is shown in purple. Binding site is located on the right-low corner, where heme group is shown in orange and iron ion in red. Residue Tyr642 is shown in black, forming a coordination bond with the iron atom of the porphyrin moiety. Val564 occupies a position in the vicinity of the metal coordination sphere without interacting with the metal. This figure was prepared with the program Pymol 0.99. The inset depicts the structure of a canonical metalloporphyrin, which is identical to heme b except that the iron atom is replaced by another metal.[43]

as IsdA.[16,17] Figure 1 shows the structure and binding conformation of the IsdH-NEAT3·Fe(III)-PPIX complex.[16] Interestingly, IsdH confers *S. aureus* some ability to evade the immune system, and thus a precise understanding of heme binding and transport in this protein could be used to develop more potent and safer vaccines against *S. aureus*.[18−20]

In a separate strategy, several research groups have reported the use of so-called non-iron metalloporphyrins, i.e., porphyrins containing metals other than iron, as antibacterial weapons. This strategy was pioneered by Stojiljkovic et al., showing that some metalloporphyrins severely arrested the growth of Gram-positive and Gram-negative pathogenic bacteria including *S. aureus*.[21] Ga(III)-PPIX was considered a particularly promising antibacterial candidate with potential to enter the clinical stage because it showed little toxicity toward human cultured cells up to concentrations 100-fold higher than those causing growth inhibition in *S. aureus*. At least two additional reports have corroborated this initial discovery in *Plasmodium falciparum* and *Porphyromonas gingivalis*, thus expanding the range of microorganisms susceptible to these porphyrin-based compounds.[22,23] The mechanism by which they exert their antimicrobial effect is not fully understood, although it has been proposed that non-iron metalloporphyrins enter bacterial cells through heme conduits, after which they cause widespread toxicity by generating reactive oxygen radicals.[21] According to the so-called "Trojan horse" hypothesis, internalization of non-iron porphyrins is facilitated by heme-import systems.[21] We investigated whether these antimicrobial compounds bind to IsdH-NEAT3, which is the first receptor of the Isd system of *S. aureus*.

Herein we report that oxidation state of the metal center of the porphyrin ring (i.e., electrostatic charge) modulates porphyrin binding to IsdH-NEAT3. We observed that affinity of porphyrins carrying metals in oxidation state (III) is higher, and binding more stable, than that of porphyrins containing metals in oxidation state (II). Interestingly, these results mirrored the reported antibacterial potency of non-iron metalloporphyrins.[21] The crystal structures of IsdH-NEAT3 in complex with Ga(III)-PPIX or Mn(III)-PPIX and the transfer assays to second receptor IsdA revealed that antibacterial porphyrins closely mimic the properties of the natural ligand heme. Overall, our results support the hypothesis that antibacterial porphyrins may utilize Isd system to penetrate inside *S. aureus* cells, at least in the initial stages of their advance toward the inner membrane of the bacteria.

EXPERIMENTAL PROCEDURES

Metalloporphyrins. Cu(II)-PPIX, Zn(II)-PPIX, Mg(II)-PPIX, Fe(III)-PPIX chloride, and Mn(III)-PPIX chloride were purchased from Frontier Scientific (Logan, UT). Ga(III)-PPIX hydroxide was synthesized following the procedure described by Nakae et al.[24]

Purification of IsdH-NEAT3. IsdH-NEAT3 comprising residues Gly-534 to Gln-664 was expressed in *Escherichia coli* Rosetta2 (DE3) cells grown in M9 minimal medium as described elsewhere.[25] Purification of IsdH-NEAT3 were carried out essentially as described previously.[16] IsdH-NEAT3 contained an N-terminal hexahistidine that was cleaved off with protease thrombin to avoid unwanted side effects. Purified IsdH-NEAT3 was obtained after a size-exclusion chromatography step using a HiLoad 16/60 superdex 200 column (GE Healthcare, Piscataway, NJ) equilibrated with 50 mM phosphate buffer at pH 7.3.

Purification of apo-IsdA. IsdA encoding residues Ala-47 to Thr-316 was amplified by PCR using KOD-Plus DNA polymerase (Toyobo, Osaka, Japan) and cloned into a pTAC-MAT-Tag-2 Expression Vector (Sigma-Aldrich, St. Louis, MO) using forward primer pTAC-IsdA 5′-AAAACTCGAGGCAA-CAGAAGCTACGAACGCAAC-3′ and reverse primer pTAC-IsdA 5′-CCCGGGAATTCTCATTCTTTAGCTTTAG-3′. IsdA devoid of heme ligand could not be purified with satisfactory yields by the same method that was employed with IsdH-NEAT3. Therefore, *Escherichia coli* RP523, a strain permeable to heme, was employed for expression of apo-IsdA.[26] *E. coli* RP523 cells were grown in terrific broth medium supplemented with ampicillin (50 μg mL^{-1}) and D-glucose 0.4% w/v, at 37 °C under anaerobic conditions (sealed bottle) at 100 rpm. Cells did not require exogenous heme to grow under these conditions.[27] When the optical density at 600 nm reached a value of 1.0, cells were supplemented with IPTG (1.0 mM) and grown for an additional 20 h at 28 °C. Purification of IsdA was carried out similarly to IsdH-NEAT3.[16] Briefly, cells were harvested, disrupted by the sonication method in a buffer containing 20 mM Tris, 200 mM NaCl, and 20 mM imidazol at pH 7.9, and centrifuged for 30 min at 40000*g*. The soluble fraction was loaded in a His-trap column (GE Healthcare, Piscataway, NJ), washed with lysis buffer containing 30 mM imidazol, and eluted with lysis buffer containing 200 mM imidazol. N-terminal polyhistidine tag was cleaved off after a 24 h treatment with the protease thrombin. Finally, purified apo-IsdA was obtained after a size-exclusion chromatography step using a HiLoad 16/60 superdex 200 column (GE Healthcare, Piscataway, NJ) equilibrated with 50 mM phosphate buffer at pH 7.3. The purified apo-IsdA protein did not contain heme as determined from the UV−vis spectrum of the protein (see, for example, Figure 8C).

Binding Selectivity. Appropriate amounts of IsdH-NEAT3 in 50 mM phosphate buffer at pH 7.3 were mixed

with a freshly prepared solution of metalloporphyrin in DMSO. Protein and porphyrin concentration were kept in all cases at molar ratio of 1:1. Fe(II)-PPIX was prepared by supplementing a solution containing the ferric form with the reducing agent $Na_2S_2O_4$ at a concentration of 5 mM. The concentration of dithionite was kept at 2 mM in all solutions containing Fe(II)-PPIX. Samples were briefly incubated before being loaded into a diethylaminoethyl sepharose (DEAE-sepharose) ionic exchange column equilibrated with 1.0 M NaCl to remove unbound (or weakly bound) metalloporphyrin. The flow-through samples were collected after this brief step and applied to a 16/60 HiLoad Superdex 200 size-exclusion chromatography column equilibrated with 50 mM phosphate buffer at pH 7.3. Real-time chromatograms were recorded at two different wavelengths: the first one corresponding to the protein (280 nm) and the second one corresponding to the Soret band of the porphyrin ligand (~400 nm region) in an AKTA Purifier System (GE Healthcare, Piscataway, NJ) equipped with multiwavelength monitor system UV-900.

Binding Isotherm. Solutions of metalloporphyrin at a concentration of 10 μM in phosphate buffer (50 mM, pH 7.3) were titrated with increasing concentrations of IsdH-NEAT3 in a manner analogous to that described previously,[15] except that we recorded UV−vis spectra of each sample instead of fluorescence emission. Binding causes an increase in the molar absorptivity coefficient of the porphyrin ligand that can be used to estimate the association constant using the equation

$$A = A_f + (A_b - A_f)((K_a[L])/(1 + K_a[L])) \quad (1)$$

where A is absorbance, A_f is absorbance of porphyrin in the absence of receptor, A_b is absorbance of bound porphyrin, K_a is the association constant, and [L] is concentration of receptor. Experimental data were fitted to eq 1 with the program Origin 7.0 (Northampton, MA) to obtain the binding constant.

Preparation of Protein Crystals. Purified IsdH-NEAT3 was mixed with 10-fold excess Ga(III)-PPIX or Mn(III)-PPIX for 1 h. Excess or weakly bound metalloporphyrin was removed by ionic exchange chromatography in a manner analogous to that described in the binding selectivity assay above. Single crystals of protein·porphyrin complexes were obtained in different precipitant solutions depending on the ligand. Crystals of IsdH-NEAT3 in complex with Ga(III)-PPIX were grown by the vapor diffusion method (hanging drop) by mixing protein·porphyrin complex at concentration of 10 mg mL^{-1} with a precipitant solution containing poly(ethylene glycol) monomethyl ether 2000 (25−29% w:v), sodium sulfate 0.2 M, and sodium acetate 0.1 M at pH 4.2. The crystals developed in 1 month to approximate dimensions of 0.2 × 0.2 × 0.1 mm^3. Crystals of IsdH-NEAT3 in complex with Mn(III)-PPIX were grown analogously in a solution containing poly(ethylene glycol) monomethyl ether 550 (30% w:v), NaCl 0.1 M, and bicine 0.1 M at pH 9.0. These crystals reached an approximate size of 0.1 × 0.1 × 0.02 mm^3 within 1 month. Suitable crystals of each complex were harvested, immersed in a solution of mother liquor supplemented with 20% v:v glycerol for a few seconds, and subsequently frozen and stored in a vessel containing liquid N_2.

Data Collection and Structure Refinement. Data collection was carried out in beamlines AR-NE3A and AR-NW12A at the Photon Factory (Tsukuba, Japan) under cryogenic conditions (100 K). X-ray fluorescence confirmed the presence of Ga atoms in the protein crystal. Diffraction images of single crystals of IsdH-NEAT3 in the complex with Ga(III)-PPIX or Mn(III)-PPIX were processed with the program MOSFLM[28] and merged and scaled with the program SCALA of the CCP4 suite[29] to a nominal resolution of 1.7 and 2.7 Å, respectively. The space group of the crystal containing Mn(III)-PPIX was confirmed to be $P2_1$ with the program HKL2000. The three-dimensional structure was determined by the method of molecular replacement using the coordinates of IsdH in complex with heme (PDB identification code 2Z6F) with the program PHASER.[30] Initial models were further refined with the programs REFMAC5[31] and COOT.[32] The average *B*-factors of the refined atoms of metalloporphyrin and protein are comparable (Table 2), which is consistent with a full occupancy of the binding pocket of the receptor. The quality of the final model was assessed with the program PROCHECK.[33] The coordinate and structure factor files corresponding to the final models have been deposited in the RCSB Protein Data Bank under accession codes 3QUG (IsdH-NEAT3·Ga(III)-PPIX complex) and 3QUH (IsdH-NEAT3·Mn(III)-PPIX complex).

Transfer to Second Receptor IsdA. Transport of metalloporphyrins from IsdH-NEAT3 to apo-IsdA was measured according to the methodology described by Liu et al.[34] Holo-IsdH-NEAT3 (porphyrin bound) and apo-IsdA (ligand free) were mixed at a concentration of 10 μM in 0.5 mL solution containing 50 mM sodium phosphate at pH 7.3 at a temperature of 25 °C for 2 or 5 min. The proteins were then separated by ion-exchange chromatography in a DEAE column. The experimental conditions were adjusted in such a way that IsdH-NEAT3, but not IsdA, binds to the affinity column. IsdA was thus recovered in the flow-through, whereas IsdH-NEAT3 was eluted with a solution containing 500 mM NaCl. The quantitative separation of the two proteins was confirmed by SDS-PAGE (results not shown). The relative amount of metalloporphyrin transferred from IsdH-NEAT3 to second receptor IsdA was estimated from the decrease of the intensity of the Soret band in the 400 nm region (Fe(III)-PPIX, 400 nm; Ga(III)-PPIX, 420 nm; and Mn(III)-PPIX, 375 nm).

RESULTS AND DISCUSSION

Non-iron metalloporphyrins are antibacterial compounds that inhibit growth of pathogenic bacteria.[21] It is believed that these porphyrins penetrate the bacterial cells through constitutive heme conduits.[21,23] Iron-regulated surface determinant (Isd) is the main heme portal in *Staphylococcus aureus*, and IsdH-NEAT3 the first receptor that heme encounters in its route to the interior of the cell. Herein we have investigated the attachment of antibacterial analogues of heme to receptor IsdH-NEAT3 because this receptor is a potential hot spot in the transportation pathway.

We first tested the ability of IsdH-NEAT3 to capture up to six different types of metalloporphyrins—Fe(III)-PPIX (heme), Ga(III)-PPIX, Mn(III)-PPIX, Cu(II)-PPIX, Mg(II)-PPIX, and Zn(II)-PPIX—by a combination of ionic-exchange chromatography and size-exclusion chromatography. NEAT3 domain was briefly incubated with each metalloporphyrin, and the mixture was passed through an ionic exchange DEAE column to remove unbound or weakly bound metalloporphyrin. Eluted fractions from DEAE column were further subjected to size-exclusion chromatography (Figure 2A). This rigorous methodology

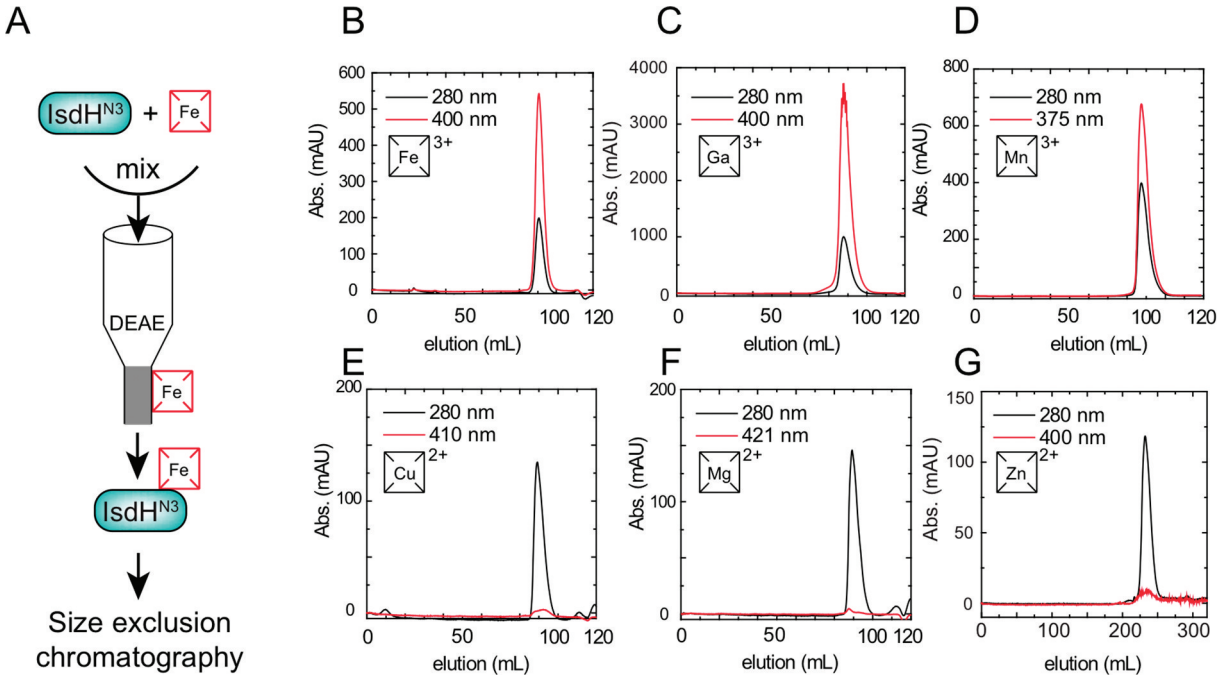

Figure 2. IsdH-NEAT3 selects porphyrins containing metal in oxidation state (III) but not oxidation state (II). (A) Experiment design. Protein was briefly incubated with metalloporphyrin, followed by anion-exchange chromatography step to remove excess or weakly bound ligand, and flow-through subjected to size-exclusion chromatography. (B–G) Size-exclusion chromatography of IsdH-NEAT3 in complex with metalloporphyrins: (B) Fe(III)-PPIX, (C) Ga(III)-PPIX, (D) Mn(III)-PPIX, (E) Cu(II)-PPIX, (F) Mg(II)-PPIX, and (G) Zn(II)-PPIX. Black traces correspond to absorbance of the protein recorded at 280 nm. Red traces correspond to absorbance of metalloporphyrin at its characteristic Soret band maximum.

identified metalloporphyrins stably bound to IsdH-NEAT3 by simply comparing their elution profile in a gel-filtration experiment. When ligand was effectively captured by the receptor, both protein and porphyrin appeared together in the same elution peak of the gel-filtration experiment. Conversely, nonspecific or weakly bound porphyrin ligands either detached during the first DEAE chromatographic step or appeared at longer retention times.[16]

Figure 2B shows a typical size-exclusion of chromatogram of IsdH-NEAT3 incubated with the natural ligand Fe(III)-PPIX. Two elution peaks appeared simultaneously at 90 mL. These peaks corresponded to protein (280 nm) and Soret band of iron porphyrin (400 nm). This experiment demonstrated that porphyrin remained attached to IsdH-NEAT3 after two chromatographic steps. Our observation is consistent with the in-vivo function of IsdH-NEAT3, which involves capturing heme molecules freed from hemoglobin by NEAT1 and NEAT2 domains.[16,35]

Among the non-iron metalloporphyrins tested, only Ga(III)-PPIX and Mn(III)-PPIX showed similar chromatographic profiles to that of Fe(III)-PPIX (Figure 2C,D). Conversely, the Soret absorption peaks of Cu(II)-PPIX, Mg(II)-PPIX, or Zn(II)-PPIX were absent from the gel-filtration chromatograms (Figure 2E–G), demonstrating that the latter porphyrins did not remain attached to the receptor. This conclusion was verified by crystallizing a sample of IsdH-NEAT3 incubated with Cu(II)-PPIX. This structure showed a binding site devoid of porphyrin molecules (results not shown). The data above revealed that porphyrins containing metals in oxidation state (III), i.e., Fe(III)-PPIX, Ga(III)-PPIX, and Mn(III)-PPIX, formed stable complexes with the receptor. In contrast, porphyrins bearing metals in oxidation state II, i.e., Cu(II)-PPIX, Mg(II)-PPIX, and Zn(II)-PPIX, did not remain bound to IsdH-NEAT3 under our experimental conditions.

The affinities of metalloporphyrins for the receptor were further investigated with a more quantitative approach. We took advantage of the hyperchromic effect that is observed upon formation of metalloporphyrin·IsdH-NEAT3 complexes. For example, Figure 3A shows that the intensity of the Soret

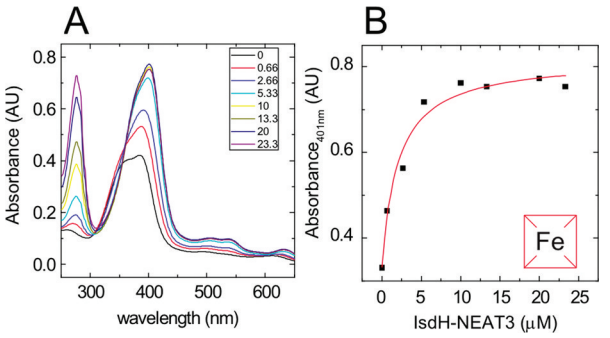

Figure 3. Binding isotherm of Fe(III)-PPIX. (A) UV–vis spectra of 10 μM heme titrated with increasing concentrations of IsdH-NEAT3 as indicated in the inset. (B) Binding isotherm. This curve was built from the values of absorbance at 401 nm shown in panel A (solid squares). The red trace corresponds to a nonlinear regression fitting of the experimental data to the equation described in the Experimental Procedures with the program Origin 7.0.

band of Fe(III)-PPIX increased when titrated with receptor. Similar observations were made with other metalloporhyrins except Zn(II)-PPIX (Figure S2). The latter metalloporphyrin showed a bimodal behavior in which absorbance signal

Table 1. Dissociation Constant and Binding Stability of Metalloporphyrins

metal in PPIX	K_D (μM)	stable[a]
Fe(III)	2.1 ± 0.5	yes
Ga(III)	2.6 ± 0.8	yes
Mn(III)	2.5 ± 0.9	yes
Cu(II)	13.5 ± 7.0	no
Zn(II)	N.A.[b]	no
Mg(II)	N.D.[c]	no
Fe(II)	N.D.	no

[a]Stable refers as to whether metalloporphyrin did or did not remain attached to IsdH-NEAT3 after the chromatographic step described in Figures 2 and 4. [b]N.A. = not applicable. [c]N.D. = not determined.

increased at first, followed by a decrease at higher concentrations of ligand. The binding isotherms (Figure 3B and Figure S2) were fitted to eq 1 as described in the Experimental Procedures (except Zn(II)-PPIX, which did not obey this binding equation). The dissociation constants presented in Table1 indicated that affinity of metalloporphyrins bearing metals in oxidation state III were comparable to each other within experimental error. Moreover, these group of porphyrins displayed ~5-fold stronger affinity than Cu(II)-PPIX.

In all these examples, the central portion of the porphyrin molecule must be positively charged (+1) when the metal exists in oxidation state III, but uncharged when metal is in oxidation state II. This argument suggested that electrostatic forces modulated the attachment of metalloporphyrin to NEAT3

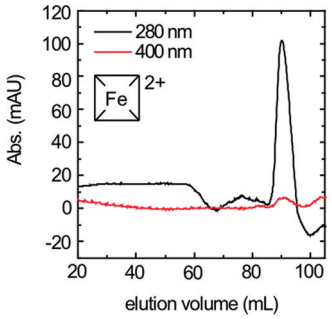

Figure 4. Reduction of Fe(III)-PPIX (ferric) to Fe(II)-PPIX (ferrous) reduced the stability of the complex with IsdH-NEAT3. Ferric porphyrin was reduced to ferrous form with 5 mM $Na_2S_2O_4$ and subjected to the same two chromatographic steps described in Figure 2.

receptor. This hypothesis was tested by reducing Fe(III)-PPIX to Fe(II)-PPIX with 5 mM sodium dithionite (Figure 4). Reduced ferrous-PPIX was subjected to the same chromatographic steps described in Figure 2. The resulting chromatogram indicated that binding stability of Fe(II)-PPIX was qualitatively similar to metalloporphyrins carrying metals in oxidation state II. This experiment reinforced the idea that electrostatic forces (via changes in oxidation state) modulated the stability of metalloporphyrin/IsdH-NEAT3 complexes.

These data were consistent with the observation made by Pluym et al. in the NEAT domain of heme-transporter IsdC.[36] These authors found that chemical reduction of IsdC·Fe(III)-PPIX with sodium dithionite led to loss of heme

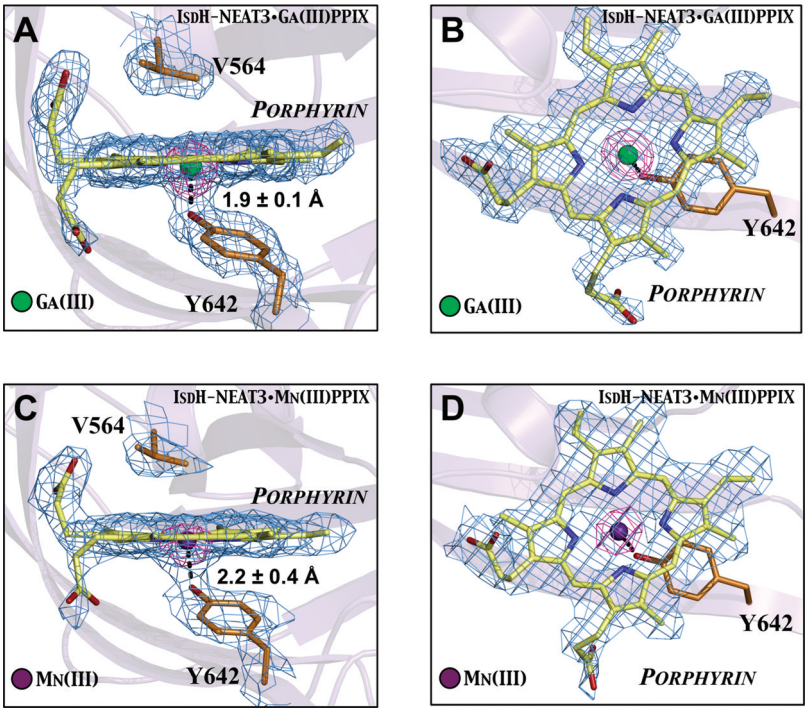

Figure 5. Electron density map of metalloporphyrins bound to IsdH-NEAT3. (A, B) Ga(III)-PPIX complex, and (C, D) Mn(III)-PPIX complex. The orientation of panels B and D differed by ~90° compared to that of panels A and C. SigmaA weighted $2F_o - F_c$ electron density maps were contoured at a level of 1.0 (blue) or 5.0 (magenta), the latter emphasizing the electron density of the metal atom. Carbon atoms belonging to the porphyrin are shown in yellow, those belonging to the protein in orange, oxygen atoms are shown in red, and nitrogen atoms are shown in blue. The large sphere depicted in the center of the porphyrin moiety corresponds to the metal, colored green and purple for Ga(III) and Mn(III), respectively. The coordination bond between Tyr642 of the protein and metal center and their average distances are also shown. In contrast, Val564 occupies a position near the metal but does not form a coordination bond. The semitransparent cartoon corresponds to the secondary structure elements of the protein.

dx.doi.org/10.1021/bi200493h | *Biochemistry* 2011, 50, 7311–7320

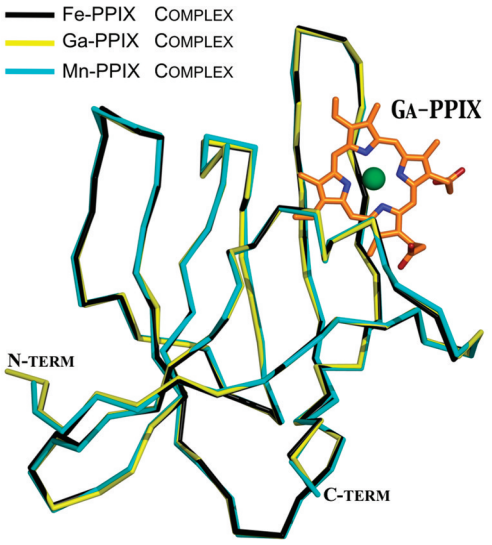

Figure 6. Crystal structures of IsdH-NEAT3 in complex with metal(III) porphyins are virtually indistinguishable from each other. Colored ribbons correspond to the main-chain traces of IsdH-NEAT3 in complex with the following: Fe(III)-PPIX (black), Ga(III)-PPIX (yellow), or Mn(III)-PPIX (blue). Ga(III)-PPIX molecule is shown to indicate the location of the binding site of the receptor. Carbon atoms of porphyrin are shown in orange. The large sphere in green corresponds to Ga(III) ion. Space group of the crystal structure of IsdH-NEAT3 in complex Fe(III)-PPIX was $P2_12_12$ and contained one molecule of protein and porphyrin in the asymmetric unit;[16] that with Ga(III)-PPIX was crystallized in space group $P2_12_12$ and contained two molecules of protein/porphyrin complex in the asymmetric unit; crystal with Mn(III)-PPIX was crystallized in space group $P2_1$ and also contained two complexes.

from the binding site of the receptor upon formation of the ferrous species. On the contrary, analogous experiments performed with IsdA-NEAT and IsdH-NEAT3 indicated that the reduced form Fe(II)-PPIX remained attached to the receptor in a six-coordinated environment upon reduction of the metal.[36,37] In other words, oxidation state of the metal in these latter two examples could be a critical property *prior* to their attachment to NEAT domain (Figure 2). However, this property alone did not determine whether porphyrin moiety is excluded or not from the binding pocket after ligand has been captured by receptor.

Table 2. Data Collection and Refinement Statistics[a]

data collection	Ga(III)-PPIX	Mn(III)-PPIX
space group	$P2_12_12$	$P2_1$
unit cell		
a, *b*, *c* (Å)	75.42, 70.12, 49.20	41.28, 75.93, 49.33
α, β, γ (deg)	90, 90, 90	90, 95.1, 90
resolution (Å)	50.0−1.70	49.1−2.70
wavelength	1.000	1.000
observations	192 786	26 563
unique reflections	28 690	8138
R_{merge}	0.089 (0.50)	0.14 (0.40)
$I/\sigma(I)$	17.0 (2.1)	6.6 (2.8)
multiplicity	6.7 (4.2)	3.3 (3.3)
completeness (%)	97.8 (83.8)	96.7 (97.0)
refinement statistics	**Ga(III)-PPIX**	**Mn(III)-PPIX**
resolution (Å)	50.0−1.70	49.1−2.70
reflections work/free	28,515/1,180	8,127/373
R_{work}/R_{free} (%)	21.4/25.7	22.4/28.6
no. atoms in asymmetric unit	2169	1947
no. protein copies	2	2
no. residues	226	224
no. PPIX ligands	2	2
no. sulfate ions	2	0
no. of glycerol molecules	2	2
no. of waters	157	33
protein *B*-factor	29.4	38.5
PPIX ligand *B*-factor	28.2	31.0
water *B*-factor	36.5	30.0
Ramachandran plot		
preferred regions (%)	98.6	98.2
allowed regions (%)	1.4	1.8
outliers (%)	0	0
rmsd bond (Å)	0.018	0.011
rmsd angle (deg)	2.0	1.23
coordinate error (Å)	0.13	0.40
PDB identification code	3QUG	3QUH

[a]Statistical values given in parentheses refer to the highest resolution bin.

More importantly, our results above revealed a good correlation between binding selectivity and relative antibacterial potency among non-iron metalloporphyrins.[21] A closer analysis of the data reported by Stojiljkovic et al. indicated that the potency of non-iron metalloporphyrins is closely related to the oxidation state of the metal. In particular, their data

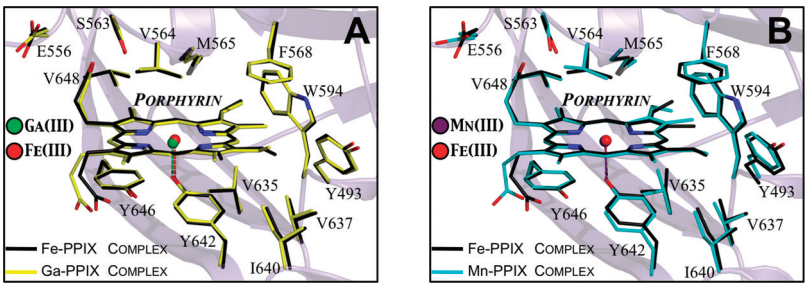

Figure 7. Detailed view of the binding pocket of IsdH-NEAT3 with metalloporphyrins bound. (A) Comparison between IsdH-NEAT3 in complex with Ga(III)-PPIX and that in complex with Fe(III)-PPIX. (B) Comparison between IsdH-NEAT3 in complex with Mn(III)-PPIX and that in complex with Fe(III)-PPIX. The two panels depict metalloporphyrins and all protein residues within a sphere of 4.0 Å from any atom of the porphyrin moiety, except Val633 which was removed from the figure to facilitate the observation of the metal center. Protein coordinates were superimposed with the program COOT.[32] Carbon atoms belonging to IsdH-NEAT3·Ga(III)-PPIX are shown in yellow, those of IsdH-NEAT3·Fe(III)-PPIX in black, and those of IsdH-NEAT3·Mn(III)-PPIX in cyan. Oxygen atoms are depicted in red and nitrogen atoms in blue.

dx.doi.org/10.1021/bi200493h | *Biochemistry* 2011, 50, 7311−7320

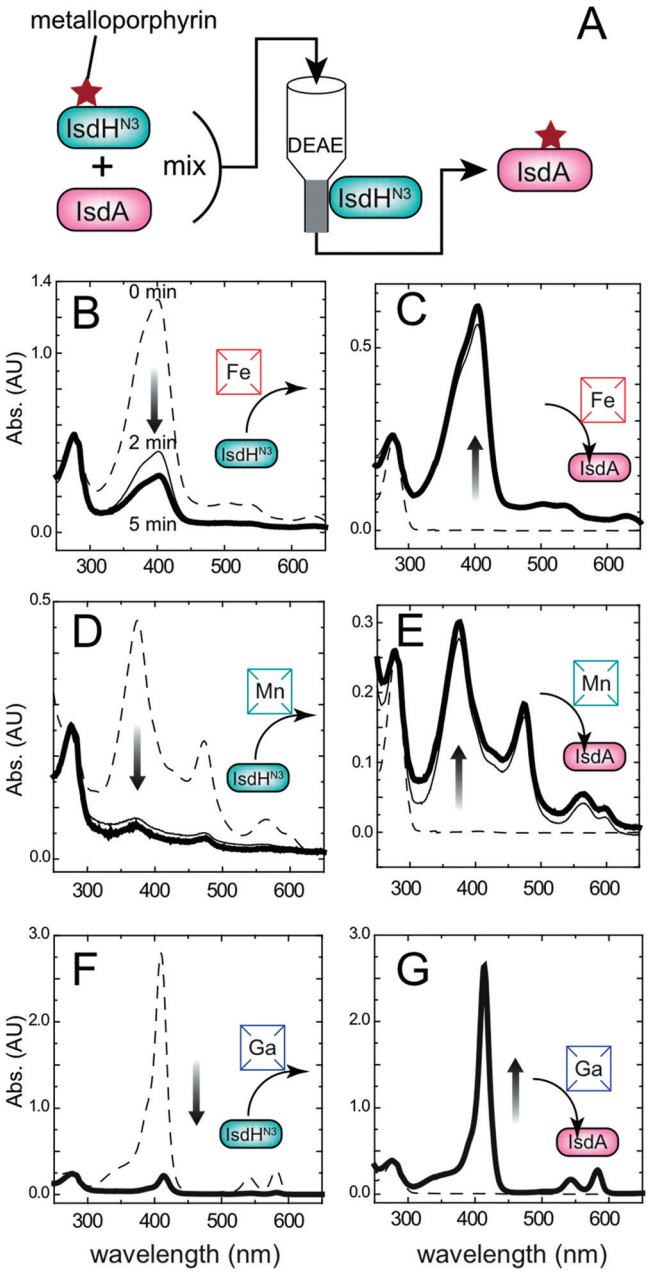

Figure 8. Transfer of metalloporphyrins from IsdH-NEAT3 to apo-IsdA. (A) Experimental design: Receptor IsdH-NEAT3 in complex with metalloporphyrin was incubated with ligand-free IsdA and the proteins separated in a DEAE ionic-exchange column. Absorption spectrum of each protein with each metal(III) porphyrin was recorded between 250 and 650 nm. Three metalloporphyrin were tested: Fe(III)-PPIX (B, C), Mn(III)-PPIX (D, E), and Ga(III)-PPIX (F, G). Panels on the left corresponded to spectra of Isd-NEAT3 after elution from the DEAE column (B, D, and F). Panels on the right corresponded to spectra of second receptor IsdA (C, E, and G). In all panels spectra after no incubation (dashed trace), 2 min incubation (fine trace) and 5 min incubation (bold trace) with apo-IsdA are shown. The arrow indicates the direction of the spectral changes upon incubation with IsdA. The amount of ligand transferred was estimated from the decrease in the intensity of the Soret band of metalloporphyrin bound to IsdH-NEAT3.

demonstrated that porphyrins bearing metals with oxidation state (III) were more potent than those bearing metals in oxidation state (II) in all three bacteria tested. Our results, using an orthogonal biophysical assay with purified samples of IsdH-NEAT3, offered a more detailed explanation of the microbiological data.

Next we determined the crystal structures of IsdH-NEAT3 in complex with Ga(III)-PPIX and Mn(III)-PPIX at a resolution of 1.7 and 2.7 Å, respectively, to observe the binding mode of non-iron porphyrins to IsdH-NEAT3 (Figure 5 and Table 2). We note that this is the first report of a crystal structure of Ga(III)-PPIX in complex with a biological macromolecule. X-ray fluorescence analysis confirmed the presence of Ga atoms in the crystals (Figure S3). The higher value of R_{merge} in the crystal of IsdH-NEAT3·Mn(III)-PPIX complex was likely caused by faster than usual radiation damage during data collection on a very thin crystal of dimensions ~0.1 × 0.1 × 0.02 mm^3. Although this unwanted effect resulted in worse statistics than those of the crystal containing Ga(III)-PPIX, it did not affect the conclusions discussed below because the final model was thoroughly validated before being deposited in the Protein Data Bank.

A closer look at the structures depicted in Figure 5 demonstrated clear electron density features in the binding pocket of IsdH-NEAT3 consistent with the presence of a metalloporphyrin molecule. Metal atoms occupied the highest electron density region in the center of the porphyrin ring. Omit electron density maps (calculated without taking into account the scattering power of the porphyrin moiety) showed essentially the same features as above (Figure S4). In both structures, Ga(III) and Mn(III) are coordinated to axial ligand Tyr642 and not to neighboring residue Val564. Continuous electron-density features and short distance between oxygen atom of Tyr642 and metal suggested that this coordination bond is critical to capture metalloporphyrin.

Comparison of atomic coordinates of IsdH-NEAT3 in complex with Fe(III)-PPIX,[16] Ga(III)-PPIX, and Mn(III)-PPIX demonstrated that all three structures were indeed nearly indistinguishable from each other. Their overall fold, secondary structure elements, stoichiometry, and relative position of the porphyrin ligand were very similar in the three structures (Figure 6). This observation was somehow surprising when considering that these crystals were grown with different precipitant and pH solutions and crystallized in different space groups with dissimilar unit-cell parameters. The root-mean-square deviation (rmsd) between main-chain atoms of IsdH-NEAT3 with Fe(III)-PPIX bound and those of the structure containing Ga(III)-PPIX was 0.21 Å, whereas that of Mn(III)-PPIX was only slightly higher (0.30 Å). These differences are undoubtedly very small and in fact only a little larger than rmsd values found within *the same* crystal structure: rmsd value between chain A and chain B in the IsdH-NEAT3·Ga(III)-PPIX complex was 0.13 Å, whereas the equivalent rmsd of the structure containing Mn(III)-PPIX was 0.20 Å.

The similarities among the three crystal structures were also found throughout the porphyrin binding pocket (Figure 7). Atomic coordinates of protein and ligand atoms as well as conformation of residues located at a distance of 4 Å or less from the porphyrin moiety did not change significantly in response to the different metals. Interestingly, the distance between axial ligand Tyr642 and metal atom of the porphyring ring is slightly shorter in Ga(III)-PPIX complex (1.9 ± 0.1 Å) than in the natural ligand Fe(III)-PPIX (2.2 ± 0.15) or Mn(III)-PPIX (2.2 ± 0.4 Å) (error corresponded to a diffraction-component precision index computed by the

dx.doi.org/10.1021/bi200493h | *Biochemistry* 2011, 50, 7311–7320

method of Cruickshank[38]). These differences were too small to affect their relative binding affinities consistent with the values shown in Table 1.

We next examined the ability of IsdH-NEAT3 to transfer the porphyrin moiety to second protein receptor IsdA (the full pathway traveled by heme is illustrated in Figure S1). We followed a similar methodology to that described by Liu et al. as indicated below.[34] Porphyrin-bound IsdH-NEAT3 (holo-IsdH) was incubated with the ligand-free form of the acceptor (apo-IsdA), followed by a brief step to separate the proteins. Each complex was analyzed by UV−vis spectrometry (Figure 8). Data showed a steep decrease of the intensity of the Soret band in samples with IsdH-NEAT3 (Figure 8B), accompanied by a dramatic increase of the intensity of the Soret band in the samples containing IsdA (Figure 8C). These results proved that a large fraction of Fe(III)-PPIX was effectively transferred from holo-IsdH to downstream receptor apo-IsdA.

Similarly, Ga(III)-PPIX and Mn(III)-PPIX were also transferred from the holo-NEAT3 donor to the apo-IsdA receptor. In all three cases, more than 85% of ligand molecules initially bound to IsdH-NEAT3 appeared attached to acceptor protein IsdA after a brief incubation period of 2 min (86% for Fe(III)-PPIX, 92% for Ga(III)-PPIX, and 97% for Mn(III)-PPIX). The amount of metalloporphyrin transferred from Isdh-NEAT3 to apo-IsdA did not increase significantly when the incubation time was extended from 2 to 5 min, indicating that transfer reaction is specific and relatively fast (faster than passive transfer in IsdA which is on the order of hours[34] and consistent with binding stability seen in Figure 2). Moreover, the transfer of porphyrin from IsdH-NEAT3 to apo-IsdA is largely irreversible as determined from the small extent of metalloporhyrin back-transfer (<20%) from IsdA to apo IsdH-NEAT3 (Figure S5).

IsdB and IsdC are also members of the Isd system possessing NEAT domains and involved in capturing, binding, and shuttling heme molecules toward the inner membrane of the cell.[13,17,39] For example, the crystal structure of IsdC displays a similar constellation of residues in the binding pocket to those of IsdH-NEAT3 including the presence of an axial tyrosine coordinating the metal.[40] IsdC-NEAT can capture Zn(II)-PPIX with μM affinity, and the solution structure of this complex resembles that with heme.[41] It will be interesting to expand the scope of our investigations to determine, for example, if oxidation state of the metal influences affinity and structure of other IsdC-NEAT·metalloporphyrin complexes.

More recently, the crystal structure of IsdB-NEAT2 in complex with heme has revealed a novel metal-coordination architecture in a NEAT domain. This structure showed that, in addition to oxygen atom of Tyr440, sulfur atom of Met362 coordinates the iron metal of heme with fractional occupancies ranging from 0.3 to 0.8.[42] In IsdH-NEAT3 this position is occupied by noncoordinating residue Val562 (Figure 5). It will be interesting to determine whether site-directed mutagenesis at this position modulates the relative affinities among metalloporphyrins in IsdH-NEAT3.

In summary, herein we have demonstrated mechanistic equivalence between antibacterial metalloporphyrins and heme in two critical steps of Isd system of *S. aureus*. The extent of interaction of metalloporphyrin with IsdH-NEAT3 receptor is correlated with antibacterial potency. And their transfer to IsdA receptor suggested that efficient transport of metalloporphyrins into the cell by this heme transport system could be essential to achieve maximum toxicity against *S. aureus*. Finally, our data highlight the attractive idea of using Isd system as a novel route to deliver these and other similar antibacterial compounds into *S. aureus*.

■ ASSOCIATED CONTENT

Ⓢ Supporting Information

Overview of Isd system (Figure S1); binding isotherms (Figure S2); X-ray fluorescence emission spectrum of Ga(III)-PPIX·IsdH-NEAT3 crystal (Figure S3); omit electron density maps of metalloporphyrins (Figure S4); and back-transfer of metal(III)-PPIX from IsdA to apo-IsdH-NEAT3 (Figure S5). This material is available free of charge via the Internet at http://pubs.acs.org.

Accession Codes

Coordinates and structure factors of IsdH-NEAT3 in complex with metalloporphyrins have been deposited in the RCSB Protein Data Bank as entries 3QUG and 3QUH.

■ AUTHOR INFORMATION

Corresponding Author

*Ph +81-3-6409-2129, Fax +81-3-6409-2129; e-mail jmmc@ims.u-tokyo.ac.jp (J.M.M.C.); Ph +81-3-5449-5316, Fax +81-3-6409-2127, e-mail tsumoto@ims.u-tokyo.ac.jp (K.T.).

Funding

This work was supported in part by a Grant-in-Aid for General Research to K.T. from the Japan Society for the Promotion of Science.

■ ACKNOWLEDGMENTS

We thank to the staff personnel at the Photon Factory in Tsukuba for their assistance during X-ray data collection.

■ ABBREVIATIONS

Isd, iron-regulated surface determinant; PPIX, protoporphyrin IX; NEAT, NEAr Transporter domain; DEAE, diethylaminoethyl cellulose; rmsd, root-mean-square deviation.

■ REFERENCES

(1) Kuehnert, M. J., Kruszon-Moran, D., Hill, H. A., McQuillan, G., McAllister, S. K., Fosheim, G., McDougal, L. K., Chaitram, J., Jensen, B., Fridkin, S. K., Killgore, G., and Tenover, F. C. (2006) Prevalence of Staphylococcus aureus nasal colonization in the United States, 2001−2002. *J. Infect. Dis. 193*, 172−179.

(2) Peacock, S. J., de Silva, I., and Lowy, F. D. (2001) What determines nasal carriage of Staphylococcus aureus? *Trends Microbiol. 9*, 605−610.

(3) Wertheim, H. F., Vos, M. C., Ott, A., van Belkum, A., Voss, A., Kluytmans, J. A., van Keulen, P. H., Vandenbroucke-Grauls, C. M., Meester, M. H., and Verbrugh, H. A. (2004) Risk and outcome of nosocomial Staphylococcus aureus bacteraemia in nasal carriers versus non-carriers. *Lancet 364*, 703−705.

(4) Lowy, F. D. (1998) Staphylococcus aureus infections. *N. Engl. J. Med. 339*, 520−532.

(5) Streit, J. M., Jones, R. N., Sader, H. S., and Fritsche, T. R. (2004) Assessment of pathogen occurrences and resistance profiles among infected patients in the intensive care unit: report from the SENTRY Antimicrobial Surveillance Program (North America, 2001). *Int. J. Antimicrob. Agents 24*, 111−118.

(6) Kollef, M. H., and Micek, S. T. (2006) Methicillin-resistant Staphylococcus aureus: a new community-acquired pathogen? *Curr. Opin. Infect. Dis. 19*, 161−168.

(7) Smith, T. L., Pearson, M. L., Wilcox, K. R., Cruz, C., Lancaster, M. V., Robinson-Dunn, B., Tenover, F. C., Zervos, M. J., Band, J. D., White, E., and Jarvis, W. R. (1999) Emergence of vancomycin resistance in Staphylococcus aureus. Glycopeptide-Intermediate Staphylococcus aureus Working Group. *N. Engl. J. Med. 340*, 493–501.

(8) Rybak, M. J., and Akins, R. L. (2001) Emergence of methicillin-resistant Staphylococcus aureus with intermediate glycopeptide resistance: clinical significance and treatment options. *Drugs 61*, 1–7.

(9) Kuklin, N. A., Clark, D. J., Secore, S., Cook, J., Cope, L. D., McNeely, T., Noble, L., Brown, M. J., Zorman, J. K., Wang, X. M., Pancari, G., Fan, H., Isett, K., Burgess, B., Bryan, J., Brownlow, M., George, H., Meinz, M., Liddell, M. E., Kelly, R., Schultz, L., Montgomery, D., Onishi, J., Losada, M., Martin, M., Ebert, T., Tan, C. Y., Schofield, T. L., Nagy, E., Meineke, A., Joyce, J. G., Kurtz, M. B., Caulfield, M. J., Jansen, K. U., McClements, W., and Anderson, A. S. (2006) A novel Staphylococcus aureus vaccine: iron surface determinant B induces rapid antibody responses in rhesus macaques and specific increased survival in a murine S. aureus sepsis model. *Infect. Immun. 74*, 2215–2223.

(10) Stranger-Jones, Y. K., Bae, T., and Schneewind, O. (2006) Vaccine assembly from surface proteins of Staphylococcus aureus. *Proc. Natl. Acad. Sci. U. S. A. 103*, 16942–16947.

(11) Kim, H. K., DeDent, A., Cheng, A. G., McAdow, M., Bagnoli, F., Missiakas, D. M., and Schneewind, O. (2010) IsdA and IsdB antibodies protect mice against Staphylococcus aureus abscess formation and lethal challenge. *Vaccine 28*, 6382–6392.

(12) Mazmanian, S. K., Skaar, E. P., Gaspar, A. H., Humayun, M., Gornicki, P., Jelenska, J., Joachmiak, A., Missiakas, D. M., and Schneewind, O. (2003) Passage of heme-iron across the envelope of Staphylococcus aureus. *Science 299*, 906–909.

(13) Grigg, J. C., Ukpabi, G., Gaudin, C. F., and Murphy, M. E. (2010) Structural biology of heme binding in the Staphylococcus aureus Isd system. *J. Inorg. Biochem. 104*, 341–348.

(14) Skaar, E. P., and Schneewind, O. (2004) Iron-regulated surface determinants (Isd) of Staphylococcus aureus: stealing iron from heme. *Microbes Infect. 6*, 390–397.

(15) Pilpa, R. M., Robson, S. A., Villareal, V. A., Wong, M. L., Phillips, M., and Clubb, R. T. (2009) Functionally distinct NEAT (NEAr Transporter) domains within the Staphylococcus aureus IsdH/HarA protein extract heme from methemoglobin. *J. Biol. Chem. 284*, 1166–1176.

(16) Watanabe, M., Tanaka, Y., Suenaga, A., Kuroda, M., Yao, M., Watanabe, N., Arisaka, F., Ohta, T., Tanaka, I., and Tsumoto, K. (2008) Structural basis for multimeric heme complexation through a specific protein-heme interaction: the case of the third neat domain of IsdH from Staphylococcus aureus. *J. Biol. Chem. 283*, 28649–28659.

(17) Tiedemann, M. T., Muryoi, N., Heinrichs, D. E., and Stillman, M. J. (2008) Iron acquisition by the haem-binding Isd proteins in Staphylococcus aureus: studies of the mechanism using magnetic circular dichroism. *Biochem. Soc. Trans. 36*, 1138–1143.

(18) Clarke, S. R., and Foster, S. J. (2008) IsdA protects Staphylococcus aureus against the bactericidal protease activity of apolactoferrin. *Infect. Immun. 76*, 1518–1526.

(19) Visai, L., Yanagisawa, N., Josefsson, E., Tarkowski, A., Pezzali, I., Rooijakkers, S. H., Foster, T. J., and Speziale, P. (2009) Immune evasion by Staphylococcus aureus conferred by iron-regulated surface determinant protein IsdH. *Microbiology 155*, 667–679.

(20) Ster, C., Beaudoin, F., Diarra, M. S., Jacques, M., Malouin, F., and Lacasse, P. (2010) Evaluation of some Staphylococcus aureus iron-regulated proteins as vaccine targets. *Vet. Immunol. Immunopathol. 136*, 311–318.

(21) Stojiljkovic, I., Kumar, V., and Srinivasan, N. (1999) Non-iron metalloporphyrins: potent antibacterial compounds that exploit haem/Hb uptake systems of pathogenic bacteria. *Mol. Microbiol. 31*, 429–442.

(22) Begum, K., Kim, H. S., Kumar, V., Stojiljkovic, I., and Wataya, Y. (2003) In vitro antimalarial activity of metalloporphyrins against Plasmodium falciparum. *Parasitol. Res. 90*, 221–224.

(23) Yukitake, H., Naito, M., Sato, K., Shoji, M., Ohara, N., Yoshimura, M., Sakai, E., and Nakayama, K. (2011) Effects of non-iron metalloporphyrins on growth and gene expression of Porphyromonas gingivalis. *Microbiol. Immunol. 55*, 141–153.

(24) Nakae, Y., Fukusaki, E. I., Kajiyama, S., Kobayashi, A., Nakajima, S., and Sakata, I. (2005) The convenient screening method using albumin for the tumor localizing property of Ga-porphyrin complexes. *J. Photochem. Photobiol., A 172*, 55–61.

(25) Tanaka, Y., Morikawa, K., Ohki, Y., Yao, M., Tsumoto, K., Watanabe, N., Ohta, T., and Tanaka, I. (2007) Structural and mutational analyses of Drp35 from Staphylococcus aureus: a possible mechanism for its lactonase activity. *J. Biol. Chem. 282*, 5770–5780.

(26) Li, J. M., Umanoff, H., Proenca, R., Russell, C. S., and Cosloy, S. D. (1988) Cloning of the Escherichia coli K-12 hemB gene. *J. Bacteriol. 170*, 1021–1025.

(27) Woodward, J. J., Martin, N. I., and Marletta, M. A. (2007) An Escherichia coli expression-based method for heme substitution. *Nature Methods 4*, 43–45.

(28) Leslie, A. G. (2006) The integration of macromolecular diffraction data. *Acta Crystallogr., Sect. D: Biol. Crystallogr. 62*, 48–57.

(29) Evans, P. (2006) Scaling and assessment of data quality. *Acta Crystallogr., Sect. D: Biol. Crystallogr. 62*, 72–82.

(30) McCoy, A. J., Grosse-Kunstleve, R. W., Adams, P. D., Winn, M. D., Storoni, L. C., and Read, R. J. (2007) Phaser crystallographic software. *J. Appl. Crystallogr. 40*, 658–674.

(31) Murshudov, G. N., Vagin, A. A., and Dodson, E. J. (1997) Refinement of macromolecular structures by the maximum-likelihood method. *Acta Crystallogr., Sect. D: Biol. Crystallogr. 53*, 240–255.

(32) Emsley, P., Lohkamp, B., Scott, W. G., and Cowtan, K. (2010) Features and development of Coot. *Acta Crystallogr., Sect. D: Biol. Crystallogr. 66*, 486–501.

(33) Laskowski, R. A., MacArthur, M. W., Moss, D. S., and Thornton, J. M. (1993) PROCHECK - a program to check the stereochemical quality of protein structures. *J. Appl. Crystallogr. 26*, 283–291.

(34) Liu, M., Tanaka, W. N., Zhu, H., Xie, G., Dooley, D. M., and Lei, B. (2008) Direct hemin transfer from IsdA to IsdC in the iron-regulated surface determinant (Isd) heme acquisition system of Staphylococcus aureus. *J. Biol. Chem. 283*, 6668–6676.

(35) Muryoi, N., Tiedemann, M. T., Pluym, M., Cheung, J., Heinrichs, D. E., and Stillman, M. J. (2008) Demonstration of the iron-regulated surface determinant (Isd) heme transfer pathway in Staphylococcus aureus. *J. Biol. Chem. 283*, 28125–28136.

(36) Pluym, M., Muryoi, N., Heinrichs, D. E., and Stillman, M. J. (2008) Heme binding in the NEAT domains of IsdA and IsdC of Staphylococcus aureus. *J. Inorg. Biochem. 102*, 480–488.

(37) Tiedemann, M. T., Muryoi, N., Heinrichs, D. E., and Stillman, M. J. (2009) Characterization of IsdH (NEAT domain 3) and IsdB (NEAT domain 2) in Staphylococcus aureus by magnetic circular dichroism spectroscopy and electrospray ionization mass spectrometry. *J. Porphyrins Phthalocyanines 13*, 1006–1016.

(38) Cruickshank, D. W. (1999) Remarks about protein structure precision. *Acta Crystallogr., Sect. D: Biol. Crystallogr. 55*, 583–601.

(39) Reniere, M. L., Torres, V. J., and Skaar, E. P. (2007) Intracellular metalloporphyrin metabolism in Staphylococcus aureus. *Biometals 20*, 333–345.

(40) Sharp, K. H., Schneider, S., Cockayne, A., and Paoli, M. (2007) Crystal structure of the heme-IsdC complex, the central conduit of the Isd iron/heme uptake system in Staphylococcus aureus. *J. Biol. Chem. 282*, 10625–10631.

(41) Villareal, V. A., Pilpa, R. M., Robson, S. A., Fadeev, E. A., and Clubb, R. T. (2008) The IsdC protein from Staphylococcus aureus

uses a flexible binding pocket to capture heme. *J. Biol. Chem. 283*, 31591−31600.

(42) Gaudin, C. F., Grigg, J. C., Arrieta, A. L., and Murphy, M. E. (2011) Unique Heme-Iron Coordination by the Hemoglobin Receptor IsdB of Staphylococcus aureus. *Biochemistry 50*, 5443−5452.

(43) Smith, L. J., Kahraman, A., and Thornton, J. M. (2010) Heme proteins--diversity in structural characteristics, function, and folding. *Proteins 78*, 2349−2368.